J. Biochem. **142,** 49–54 (2007)
doi:10.1093/jb/mvm099

Marked Difference Between Self-aggregations of First and Fourth Repeat Peptides on Tau Microtubule-binding Domain in Acidic Solution

Fumie Mizushima[1], Katsuhiko Minoura[1,*], Koji Tomoo[1], Miho Sumida[2], Taizo Taniguchi[2] and Toshimasa Ishida[1]

[1]*Osaka University of Pharmaceutical Sciences, 4-20-1 Nasahara, Takatsuki, Osaka 569-1094; and*
[2]*Behavioral and Medical Sciences Research Consortium, 2-5-7 Tamachi, Akashi, Hyogo 673-0025, Japan*

Received March 2, 2007; accepted April 17, 2007; published online April 24, 2007

The heparin-induced self-aggregation behaviours of four repeat peptides (R1–R4) in an acidic solution (pH = 4.5) were investigated by fluorescence and circular dichroism (CD) measurements and compared with those in a neutral solution (pH = 7.5). In contrast with the self-aggregation–resistive behaviours of the R1 and R4 repeat peptides in the neutral solution, the R4 peptide formed a filament similarly to the R2 and R3 peptides in the acidic solution, whereas the R1 peptide still showed resistive behaviour for filament formation. This is the first report on the markedly different self-aggregation behaviours of the first and fourth repeat peptides on tau microtubule-binding domain.

Key words: conformational transition, filament formation, microtubule-binding domain, repeat peptide, tau.

Abbreviations: AD, Alzheimer's disease; CD, circular dichroism; His, histidine; MBD, microtubule-binding domain; HPLC, high pressure liquid chromatography; 3RMBD, three-repeated MBD; 4RMBD, four-repeated MBD; MT, microtubule; PHF, paired helical filament; ThS, thioflavin S.

Alzheimer's disease (AD) is the most common cause of dementia among the elderly. AD is accompanied by a number of structural and metabolic alterations in the brain and is characterized by two pathognomonic lesions: extracellular deposits of β-amyloid in neuritic plaques and intracellular neurofibrillary tangles. The latter is composed of bundles of paired helical filaments (PHFs), which are abnormal aggregates of tau (*1*).

Tau protein is normally found on axonal microtubules (MTs) and plays an important role in the regulation of MT formation and stabilization (*2*). This MT-associated tau is a highly soluble protein and hardly shows any tendency to assemble under physiological conditions. However, it dissociates from MT and aggregates to form insoluble PHF fibers in the brain of AD patients (*3*, *4*). Because these fibers are toxic to neurons owing to the damage they cause to the cell interior, many studies have been performed *in vivo* as well as *in vitro* to clarify tau PHF formation mechanism (*5–9*) and to find the inhibitor of tau fibrillization (*10*, *11*). However, further studies are needed to clarify the exact mechanism because of the lack of information on the PHF structure at the atomic level and of the formation mechanism of a fully established filament.

The microtubule-binding domain (MBD) of tau consists of three or four imperfect 31–32-residue repeats (names as 3RMBD or 4RMBD, respectively) (Fig. 1) and forms the core of tau PHF (*12–14*), and is capable of self-assembling into a filament similar to that of full-length tau *in vitro* (*15*). Therefore, the analysis of the self-assembly mechanism of MBD repeat peptides could provide the needed information on the effective method of inhibiting the PHF formation of tau. In a series of studies for elucidating which part and what structural change in the tau MBD domain are most involved in its transformation into a pathological entity, recently, we have investigated the *in vitro* heparin-induced initial self-aggregation feature of each repeat peptide (R1–R4) in a neutral solution (pH = 7.5) (*7*), and clarified the high-promoting abilities of the R2 and R3 peptides at the extension and nucleation steps of filament formation, respectively, together with the high-resistive abilities of the R1 and R4 peptides for their self-aggregations.

It is important to uncover the self-aggregation behaviours of the R1 and R4 peptides irrespective of their low self-aggregation abilities, because 3RMBD or 4RMBD, which includes the R1 and R4 peptides, participates in the intact PHF formation of tau. The sequences of the R1–R4 repeats (Fig. 1) show that the theoretical pI of the R4 peptide (6.73) is significantly lower than the other pIs (R1 = 9.83, R2 = 9.52 and R3 = 9.52). Thus, to investigate the pH-dependent aggregation behaviour of the R4 peptide and to compare this behaviour with those of the R1–R3 peptides, we investigated the *in vitro* heparin-induced aggregation features of four repeat peptides in an acidic buffer (pH 4.5) by fluorescence, circular dichroism (CD) spectroscopy, and electron microscopy (EM).

MATERIALS AND METHODS

Peptides and Chemicals—R1–R4 peptides (Fig. 1B) were synthesized using the usual solid-phase synthesizer.

*To whom correspondence should be addressed. Tel: 072-690-1068, Fax: 072-690-1068, E-mail: minoura@gly.oups.ac.jp

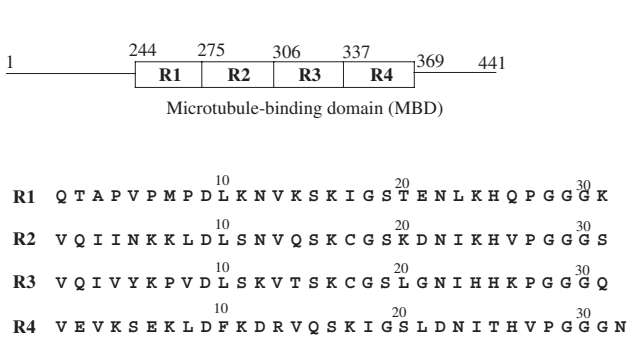

Fig. 1. **(A) Schematic of human full-length tau protein including four-repeated MBD and (B) amino acid sequences of R1–R4 repeats.** The regions from the first repeat to the fourth repeat in MBD are named R1–R4, respectively. The number of amino acid residues in (A) refers to the longest isoform of the human protein tau (441 residues).

The peptides obtained in the lyophilized form were characterized by mass spectrometry and determined to be >95.0% pure by reverse-phase high pressure liquid chromatography (HPLC). Heparin (average molecular weight = 6,000) and thioflavin S (ThS) were purchased from Sigma Co. The other commercially available materials used were of reagent grade or higher.

ThS Fluorescence Measurement—Solutions of the R1–R4 peptides each at 25 μM were prepared using 5 mM acetate buffer (pH 4.5), and 10 μM ThS was added to each solution. Fluorescence intensity was measured using a JASCO FP-770F spectrometer with a 2-mm quartz cell maintained at 25°C using a circulating water bath. The kinetics of each peptide aggregation was analysed as a function of heparin concentration by recording the time course of fluorescence intensity with excitation at 440 nm and emission at 500 nm. The excitation and emission slit widths were set at 10 nm. The background fluorescence of the sample was subtracted when necessary.

CD Measurement—Solutions of the R1–R4 peptides each at 25 μM were prepared using 5 mM acetate buffer (pH 4.5), and an optimal concentration of heparin (6.25 μM), which was pre-determined by the ThS fluorescence measurement, was added to induce the aggregation of each sample solution. All measurements were taken at 25°C using a JASCO J-820 spectrometer with a cuvette having a 2 mm path length. For each experiment under N_2 gas flow, the measurement from 190 nm to 250 nm was repeated eight times and the results were summed. Then, molar ellipticity was determined after normalizing peptide concentration. The same measurement was repeated at least three times using newly prepared samples, and the reproducibility of the results was confirmed. Data are expressed in terms of mean residue ellipticity [θ] in deg $cm^2\,dmol^{-1}$.

EM Measurement—Solutions of the R1–R4 peptides each at 25 μM were prepared and mixed with 6.25 μM heparin in 5 mM acetate buffer (pH 4.5). Each solution was then incubated at 37°C for 100 min. Copper grids (600 mesh) were used for negative-staining EM. A drop of each of the protein solutions and 2% uranyl acetate was placed on the grid. After 2 min, excess fluid was removed from the grids. Negative-staining EM was performed using an electron microscope (Hitachi Co.) operated at 75 kV.

RESULTS

Heparin-concentration Dependence of Self-aggregation of Each Peptide—The optimal heparin concentration for the self-aggregation of each of the R1–R4 peptides in the acid buffer (pH 4.5) was investigated by monitoring the ThS fluorescence intensity. The time course of fluorescence intensity as a function of heparin concentration is shown in Fig. 2, and the parameters for characterizing the aggregation profile are given in Table 1, in which those in the neutral buffer (pH=7.5) are also given for comparison; these values were measured according to the method reported in a previous paper (*16*). Previously, we reported that the aggregation rate in the neutral buffer is in the order of R3 ≫ R2 and R1 = R4 = 0, regardless of the different concentration of the peptide or heparin used in the experiment (*16*, *17*). However, the present result in the acidic solution is different from that in the neutral solution. It is interesting that the R4 peptide shows a heparin concentration-dependent filament formation profile similar to those of the R2 and R3 peptides, whereas the R1 peptide does not form any filament. Because the pI of the R4 peptide is considerably smaller than that of each of the R1–R3 peptides and its atomic charge distribution is different from that of each of the R1–R3 peptides, such filament formation may be largely related to the non-inonization and disposition of acidic amino acid residues in the R4 peptide; the numbers of polar and basic amino acids in the R4 peptide are almost the same as those of each of the R1–R3 peptides (Fig. 1). However, the notable difference between the filament formation abilities of the R1 and R2/R3 peptides indicates that the polar and basic amino acid residues characterizing each repeat peptide also play an important role in the self-aggregation.

The optimal concentration of heparin was approximately near 6.25 μM with respect to the 25 μM repeat peptide, which corresponds to the molar ratio of 0.25 (1 : 4) and is slightly larger than that in the neutral solution (~0.1). As shown in Table 1 and Fig. 2, the acidic environment shortens the lag time for the filament formation and the saturation time for the self-aggregation, and enhances the filament formation rate considerably, consequently leading to a common filament formation pattern regardless of the different peptide sequences of each of the R2–R4 peptides; this is in contrast with the sequence-dependent patterns of the R2 and R3 peptides in the neutral environment (*16*).

CD Spectral Change of Repeat Peptide Accompanied by Self-aggregation—To monitor the conformational transition of each peptide accompanied by filament formation in the acidic solution, CD spectral change was measured as a function of reaction time, where 6.3 μM heparin was added to each 25 μM peptide solution. The time–CD spectrum profiles are shown in Fig. 3, and the parameters for characterizing their conformational transitions are given in Table 2, in which those in the neutral solution are also given for comparison.

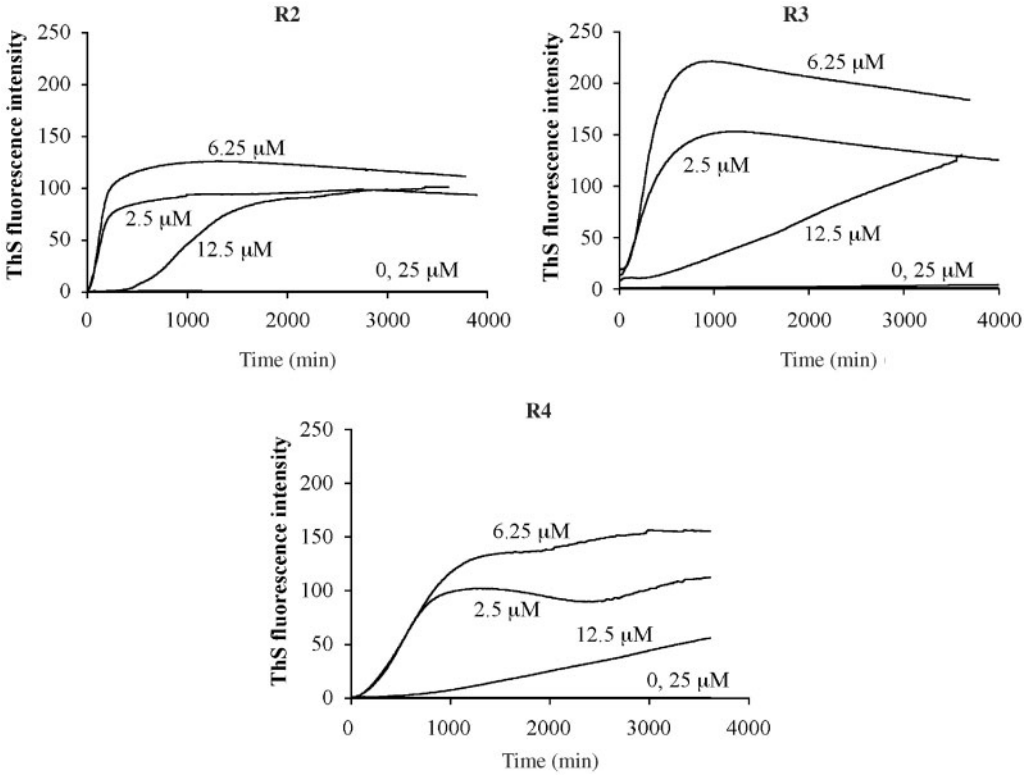

Fig. 2. **Heparin concentration dependence of ThS fluorescence intensities accompanying self-aggregations of R2–R4 peptides (25 μM) in 5 mM acetate buffer (pH 4.5).** No fluorescence intensity was observed for the R1 peptide regardless of the concentration of heparin.

Table 1. **Parameters for defining characteristic of ThS fluorescence intensity increasements accompanying self-aggregations of R1–R4 peptides (25 μM).**

Repeat peptide	pH	Lag time for filament formation	Optimal concentration of heparin	Molar ratio of heparin/peptide	Aggregation rate (intensity/time)[a]	Saturation time
R1[b]	4.5	—	—	—	—	—
R2	4.5	~0 min	6.25 μM	0.25	40 min^{-1}	~15 min
R3	4.5	~0 min	6.25 μM	0.25	26 min^{-1}	~14 min
R4	4.5	~3 min	6.25 μM	0.25	8 min^{-1}	~21 min
R1[b]	7.6	—	—	—	—	—
R2	7.6	~6 h	2.5 – 6.25 μM	0.1–0.25	8 h^{-1}	~28 h
R3	7.6	~0 h	≥2.5 μM	≥0.1	29 h^{-1}	~9 h
R4[b]	7.6	—	—	—	—	—

[a]The value denotes the slope of the linearly increasing ThS fluorescence intensity with respect to the reaction time at an optimal concentration of heparin concentration.
[b]No fluorescence intensity.

Characteristically, all the CD spectra of the R2–R4 peptides showed a common conformational change from the native random structure to the β-sheet structure without any notable contributions of other secondary structures in the acidic solution; the presence of an isochromatic point (207 or 209 nm) indicates the transition between two secondary structural components. From Table 2, it is shown that the acidic condition reduces the lag time for initiating the conformational transition and the completion time of the conformational transition significantly. It is noteworthy that the R3 peptide in the neutral solution, which shows the highest self-aggregation ability, also undergoes the two-state conformational transition similarly to the case in the acidic solution, suggesting a major filament formation pathway. This is in contrast with the case of the R2 peptide in the neutral solution (*16*), wherein the features such as the long lag time, the lack of an isochromatic point, and the contribution of the α-helix structure indicate a different route of filament formation.

One of the most interesting features is that the R1 peptide is the most resistive in term of filament formation, the conformation of which remained unchanged and it maintained the same random structure in both the acidic and neutral solutions.

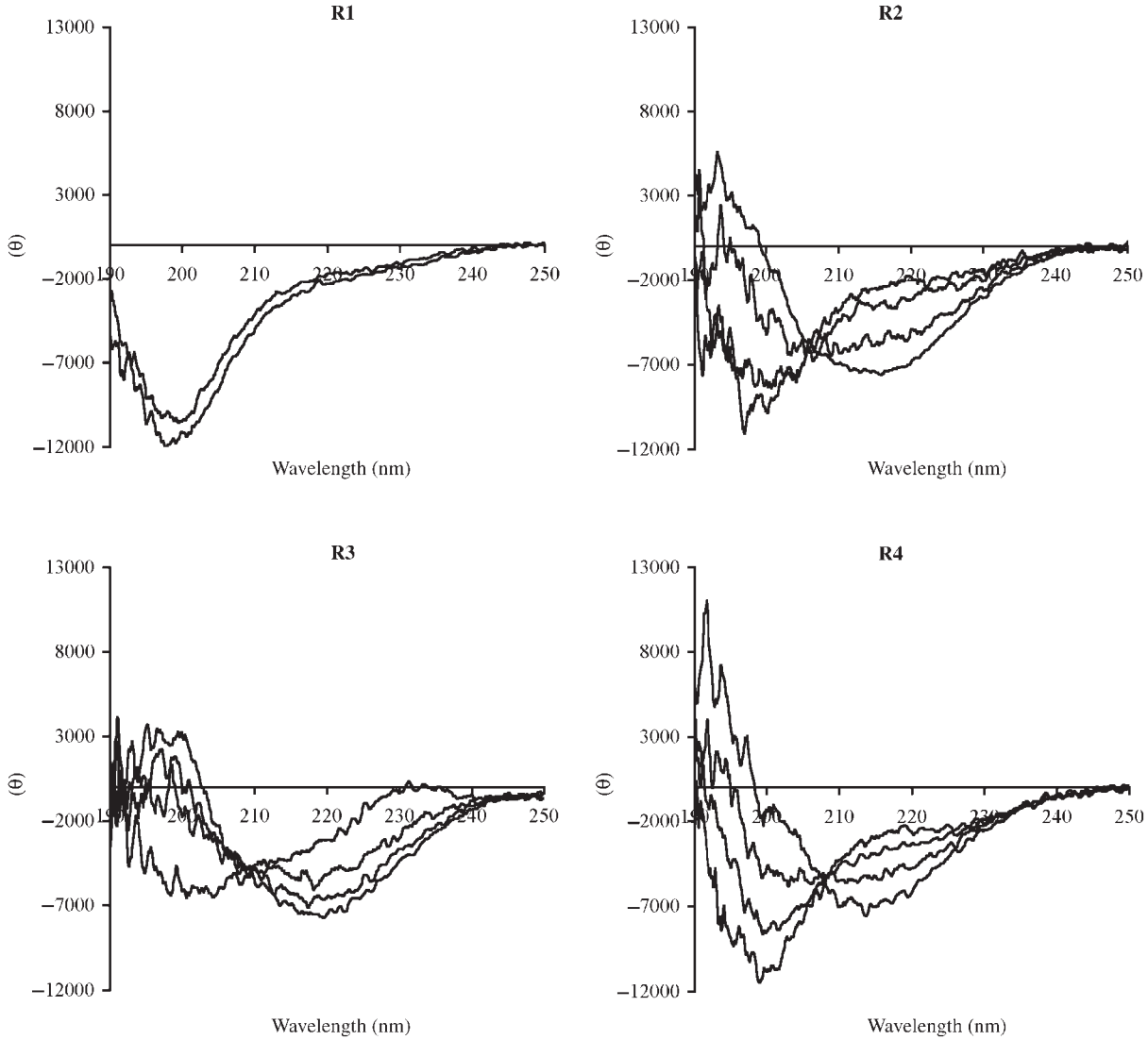

Fig. 3. **Time-resolved CD spectral changes of R1–R4 peptides (25 μM) after addition of optimal heparin concentration (6.25 μM) to 5 mM acetate buffer (pH 4.5).** Curves of the R2–R4 peptides from top to bottom at the 220 nm correspond to 0, 10, 20, 60 and 90 min after the addition of heparin, respectively, whereas those of the R1 peptide was essentially unchanged during the measurement.

Table 2. **Parameters for characterizing time-resolved CD spectral changes accompanying self-aggregations of R1–R4 peptides (25 μM) at 6.25 μM heparin.**

Repeat peptide	pH	Lag time for starting transition	Time for completion of transition	Isochromatic point
R1[a]	4.5	—	—	—
R2	4.5	~10 min	~1 h	207 nm
R3	4.5	~5 min	~10 min	209 nm
R4	4.5	~10 min	~1.5 h	209 nm
R1[a]	7.6	—	—	—
R2	7.6	~10 h	~38 h	ND
R3	7.6	~0.25 h	~2.5 h	209 nm
R4[a]	7.6	—	—	—

[a]No fluorescence intensity.

Electron Micrographs—Figure 4 shows the EM images of the heparin-induced fibrils of the R2–R4 peptides in the acidic buffer (pH = 4.5). As compared with the four-repeated MBD fibrils (*18*), those of the R2–R4 peptides showed the non-physiological morphology of thin and straight filaments, probably due to the short peptide length and the high speed of assembly. However, a notable difference was observed in their shapes, that is, the R2 peptides formed short and segmented filaments, whereas the R3 and R4 peptides formed the thin and the relatively long filaments. On the other hand, the filament formations of the R2–R4 peptides may be carried out in two steps: first, sphere-like aggregates commonly form at the early stage in a short time; second, these aggregates transform into filamentous forms.

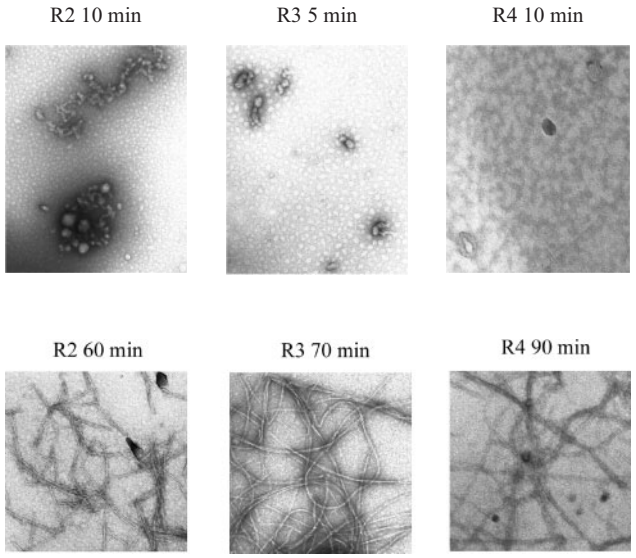

Fig. 4. **Negative-staining EM images of time-resolved filament formations of R2, R3 and R4 peptides (25 μM) as induced by heparin at 6.25 μM.** Respective samples were negatively stained with 2% uranyl acetate.

DISCUSSION

To consider any therapy for suppressing the progress of AD, it is critical to determine the molecular structure that is primarily responsible for the pathological aggregation of tau. In particular, it is important to determine the conformation of initiating filament formation. Previously, we reported that the intermediate conformation of 4RMBD in the transition from the native soluble form to its filamentous PHF structure participates importantly in accelerating the transition (*17*); Chirita *et al*. (*19*, *20*) has also reported the importance of an intermediate structure in tau filament formation. This emphasizes the importance of the intermediate structure as an activation or nucleation state, because tau filament formation can be divided into the following steps: activation →nucleation → extension → PHF formation. Using the R1–R4 peptides, and three- and four-repeated MBDs, recently, we investigated their conformational changes during the filament formation progress in a physiological neutral solution and reported the importance of the R2 and R3 repeat moiety of MBD in terms of filament formation (*16*). On the other hand, the participation of the R1 and R4 peptides in the intact PHF formation of tau, irrespective of their low self-aggregation abilities in a neutral solution, let us to investigate the heparin-induced self-aggregation behaviors of the R1 and R4 peptides in an acidic solution (pH = 4.5), together with the pH-dependence of conformational transitions of the R2 and R3 peptides in the filament formation.

A 1 : 4 molar ratio of heparin : repeat peptide has been reported to be the most effective ratio for inducing tau aggregation, because the negative charges of one heparin (average molecular weight of 3,000 Da) can neutralize the positive charges of four tau molecules in a 1 : 4 complex (*9*). Similarly, this charge-dependent optimal molar ratio was observed to induce the filament formations of the R2–R4 peptides in the acidic solution. Because the lag time and saturation time for the self-aggregation were dependent on the heparin concentration of less than 6.26 μM and the heparin concentration of more than 6.25 μM suppressed the extensions of the filaments of these peptides, an optimal amount of heparin is necessary for the completion of the activation and nucleation steps of the filament formations of the R2–R4 peptides; the polyanion such as heparin is considered to arrange the repeat peptides *via* the electrostatic interactions, so as to make easy the transformation of their random conformations to the filamentous sheet structures (*7*).

On the other hand, the parameters for characterizing the ThS fluorescence profiles (Table 1) showed that the acidic solution has a high potency for transforming repeat peptides into the filamentous state, where the lag time and saturation time for filament formation are both shortened significantly. Interestingly, the filament formation of the R4 peptide was observed for the first time in an acidic solution. Because the pI of the R4 peptide is considerably smaller than those of the other peptides owing to five excess acidic amino acid residues of the R4 peptide, the non-ionization of these residues in the acidic solution may weaken the electrostatic effect of basic amino acids and strengthen the hydrophobic interactions between the peptides, thus leading to the enhanced self-aggregation state of the R4 peptide. In contrast, the R1 peptide showed no detectable filament formation in the acidic solution as well as in the neutral solution. Because the population ratio of hydrophobic, polar, basic and acidic residues is not very different among the R1–R3 peptides, the dimer formation of repeat peptides *via* an intermolecular disulfide bond formation, which is possible only for the R2 and R3 peptides, could be the reason why the R2 and R3 peptides could undergo distinct filament formations both in the neutral and acidic solutions; it is generally believed that the tau dimer is the building block for filament formation (*21*, *22*).

To monitor the structural change of each repeat peptide from its native soluble and unfolded form to its heparin-induced filament form, the CD spectra of the peptides were measured as a function of time after the addition of an optimal heparin concentration. Because the times required for initializing and saturating the CD spectral changes were nearly parallel to those in the case of the ThS fluorescence profiles (Fig. 2), the CD spectral changes shown in Fig. 3 would reflect the structural changes accompanying the filament formations of the peptides. It is generally accepted that the presence of an isochromatic point during a spectral change is a sign of the transition between two structural components. Thus, the CD profiles showed that the filament formations of the R2–R4 peptides are processed via conformational transition from the random structure to the β-sheet structure without any specific contributions of other secondary structures. This is different from the case in the neutral solution (*16*): the R1 and R4 peptides showed no notable filament formations, and the conformation of the R2 peptide showed a synchronized transition from the α-helix and unfolded structures to the β-sheet structure and was considerably different from the conformational transition of the R3 peptide from the

random structure to the β-sheet structure. The fact that the conformational transition from the random structure to the β-sheet structure commonly and easily proceeds in the acidic solution regardless of the different sequences of the R2–R4 peptides may indicate that this conformational transition pathway is the most direct and compulsory pathway for filament formation.

The EM measurements of the R2–R4 peptides showed the formation of common sphere-like cakes before the filament formation. The time-resolved fluorescence and CD measurements suggest that these cakes correspond to the intermediate structure between the initial and transformed structures and may consist of mixed structures of unfolded and β-sheet structural peptide conformations.

The PHF–tau is hyperphosphorylated at the Thr and Ser residues, particularly at the Ser–Pro or Thr–Pro motifs in the basic proline-rich sites (*3*). Because the MBD region of tau is flanked upstream by this proline-rich region and downstream by an another basic stretch also containing several prolines, it is obvious that the repeat peptides in MBD are largely influenced by the acidic phosphate groups. At present, two key roles are considered as the biological meaning of tau phosphorylation in early stage disease (*8*), *i.e*., (i) the modulation of tau/microtubule equilibrium to raise intracellular concentration of free tau, leading to the formation of amorphous aggregates and assembly and (ii) the stabilization of filaments once nucleated, thereby shifting equilibrium toward the fibrillized state. The present result further adds a new biological meaning, *i.e*. the phosphate-promoted molecular assembly of R2–R4 repeat peptides. The function of R1 peptide may be important for the binding of MBD with microtubule (*23*), because the R1 peptide is still resistive for the filament formation in both the neutral and acidic solutions. In conclusion, this is the first report on the marked different self-aggregation behaviours of the first and fourth repeat peptides on tau microtubule-binding domain and would be important on considering the function of each repeat peptide for the filament formation of tau MBD.

REFERENCES

1. Lee, V.M., Goedert, M., and Trojanowski, L.Q. (2001) Neurodegenerative tauopathies. *Annu. Rev. Neurosci.* **24**, 1121–1159
2. Goedert, M., Jakes, R., Spillantini, M.G., and Crowther, R.A. (1994) *Microtubules* (Hyams, J. and Lloyd, C., eds.) pp. 183–200 Wiley-Liss, Inc., New York
3. Friedhoff, P., von Bergen, M., Mandelkow, E.-M., and Mandelkow, E. (2000) Structure of tau protein and assembly into paired helical filaments. *Biochim. Biophys. Acta* **1502**, 122–132
4. Buee, L., Bussiere, T., Buee-Scherrer, V., Delacourte, A., and Hof, P.R. (2000) Tau protein isoforms, phosphorylation and role in neurodegenerative disorders. *Brain Res. Brain Res. Rev.* **33**, 95–130
5. Goux, W.J. (2002) The conformations of filamentous and soluble tau associated with Alzheimer paired helical filaments. *Biochemistry* **41**, 13798–13806
6. Gamblin, T.C., Berry, W., and Binder, L.I. (2003) Modeling tau polymerization in vitro: a review and synthesis. *Biochemistry* **42**, 15009–15017
7. Tomoo, K., Yao, T.-M., Minoura, K., Hiraoka, S., Sumida, M., Taniguchi, T., and Ishida, T. (2005) Possible role of each repeat structure of the microtubule-binding domain of the tau protein in *in vitro* aggregation. *J. Biochem.* **138**, 413–423
8. Kuret, J., Chirita, C.N., Congdon, E.E., Kannanayakal, T., Li, G., Necula, M., Yin, H., and Zhong, Q. (2005) Pathways of tau fibrillization. *Biochim. Biophys. Acta* **1739**, 167–178
9. von Bergen, M., Barghorn, S., Biernat, J., Mandelkow, E.-M., and Mandelkow, E. (2005) Tau aggregation is driven by a transition from random coil to beta sheet structure. *Biochim. Biophys. Acta* **1739**, 158–166
10. Pickhardt, M., Gazova, Z., von Bergen, M., Khlistunova, I., Wang, Y., Hascher, A., Mandelkow, E.-M., Biernat, J., and Mandelkow, E. (2005) Anthraquinones inhibit tau aggregation and dissolve Alzheimer's paired helical filament *in vitro* and in cells. *J. Biol. Chem.* **280**, 3628–3635
11. Necula, M., Chirita, C.N., and Kuret, J. (2005) Cyanine dye N744 inhibits tau fibrillization by blocking filament extension: implications for the treatment of tauopathic neurodegenerative diseases. *Biochemistry* **44**, 10227–10237
12. Wischik, C.M., Novak, M., Edwards, P.C., Klug, A., Tichelaar, W., and Crowther, R.A. (1988) Structural characterization of the core of the paired helical filament of Alzheimer disease. *Proc. Natl Acad. Sci. USA* **85**, 4884–4888
13. Perez, M., Valpuesta, J.M., Medina, M., Montejo de Garcini, E., and Avila, J. (1996) Polymerization of τ into filament in the presence of heparin: the minimal sequence required for τ–τ interaction. *J. Neurochem.* **67**, 1183–1190
14. Friedhoff, F., Von Bergen, M., Mandelkow, E.-M., and Mandelkow, E. (1998) A nucleated assembly mechanism of Alzheimer paired helical filaments. *Proc. Natl Acad. Sci. USA* **95**, 15712–15717
15. Crowther, R.A., Olesen, O.F., Jakes, R., and Goedert, M. (1992) The microtubule binding repeats of tau protein assemble into filaments like those found in Alzheimer's disease. *FEBS Lett.* **309**, 199–202
16. Mizushima, F., Minoura, K., Tomoo, K., Sumida, M., Taniguchi, T., and Ishida, T. (2006) Fluorescence-coupled CD conformational monitoring of filament formation of tau microtubule-binding repeat domain. *Biochem. Biophys. Res. Commun.* **343**, 712–718
17. Hiraoka, S., Yao, T.-M., Minoura, K., Tomoo, K., Sumida, M., Taniguchi, T., and Ishida, T. (2004) Conformational transition state is responsible for assembly of microtubule-binding domain of tau protein. *Biochem. Biophys. Res. Commun.* **315**, 659–663
18. Yao, T.-M., Tomoo, K., Ishida, T., Hasegawa, H., Sasaki, M., and Taniguchi, T. (2003) Aggregation analysis of the microtubule binding domain in tau protein by spectroscopic methods. *J. Biochem.* **134**, 91–99
19. Chirita, C.N. and Kuret, J. (2004) Evidence for an intermediate in tau filament formation. *Biochemistry* **43**, 1704–1714
20. Chirita, C.N., Congdon, E.E., Yin, H., and Kuret, J. (2005) Triggers of full-length tau aggregation: a role for partially folded intermediates. *Biochemistry* **44**, 5862–5872
21. Schweeers, O., Mandelkow, E.M., Biernat, J., and Mandelkow, E. (1995) Oxidation of cysteine-322 in the repeat domain of microtubule-associated protein tau controls the *in vitro* assembly of paired helical filaments. *Proc. Natl Acad. Sci. USA* **92**, 8463–8467
22. Bhattacharya, K., Rank, K.B., Evans, D.B., and Sharma, S.K. (2001) Role of cysteine-291 and cysteine-322 in the polymerization of human tau into Alzheimer-like filaments. *Biochem. Biophys. Res. Commun.* **285**, 20–26
23. Devred, F., Douillard, S., Briand, C., and Peyrot, V. (2002) First tau repeat domain binding to growing and taxol-stabilized microtubules, and serine 262 residue phosphorylation. *FEBS Lett.* **523**, 247–251